SAND2016-7636R

Sandia National Laboratories

Operated for the U.S. Department of Energy's
National Nuclear Security Administration
by **Sandia Corporation**

Albuquerque, New Mexico 87185

date: August 1st, 2016

to: Mr. Jon Hardwick, University of Exeter

from: Steven Gomez (Org. 01556), Richard Jensen (Org. 06914) and Jason Heath (Org. 06914)

subject: An Investigation of DTOcean Foundation and Anchor Systems, Part 2

---

1. Introduction

This memo documents the mechanical loading analysis performed on the second set of DTOcean program WP4 foundation and anchor systems submodule design iterations [4]. Finite Element Analysis (FEA) simulations were performed to validate design requirements defined by Python based analytic simulations of the WP4 program Naval Facilities Engineering Command (NAVFAC) tool. This FEA procedure focuses on worst case loading scenarios on shallow gravity foundation and pile anchor designs produced by WP4. These models include a steel casing and steel anchor with soft clay surrounding the steel components respectively.

Model development was created based on a WP4 module which provided soil and foundation system material properties, basic anchor system geometry, as well as boundary conditions on the soil. Four different cases were run using the WP4 program to calculate the aforementioned parameters assuming the same soft clay soil foundation for the shallow gravity foundation and pile anchor designs. The simulations implemented different loading scenarios and geometry on the varying anchor system geometry. The dummy scenario is based on a 10x fixed tidal turbines, loosely based on the HS1000 turbine. The environmental conditions on the tidal turbines were computed by WP4 and translated into mooring line loads that were then used by WP4 to select the required size and geometry of the shallow gravity foundation and pile anchor. The WP4 input files are attached to the memo in the file named foundationvalidation.xlsx. The WP4 input files were created and run by University of Exeter. Additionally, WP4 module output is also included in the attached file. The files included a total of five runs, each a combination of differing soil type and foundation type as shown in Table 1. Within each run, there were four different line loads. The WP4 output, foundation/anchor geometries, soil types, and

structure loads, were used as the input parameters for the FEA simulations. Due to time constraints, two different foundation types resting on soft clay were analyzed; Run 2 (pile foundation on soft clay) and Run 5 (shallow foundation resting on soft clay).

Table 1: WP4 module simulations

Set Up	Soil Type	Foundation Type
Run 1	Loose Sand	Pile
Run 2	Soft Clay	Pile
Run 3	Hard rock	Pile
Run 4	Loose Sand	Shallow Foundation
Run 5	Soft Clay	Shallow Foundation

The results from this study will be used to inform the DTOcean development program by providing an assessment as to whether the foundation designs will adequately support the specified load requirements. This document will cover the meshing process (including geometry simplification) as well as a look at the simulation/modeling approach. The simulation naming convention herein will reflect the RunX LineY format output by the WP4 module. For example, the Run 5 Line 2 simulation will be abbreviated R5L2.

2. Finite Element Model

CUBIT, the Sandia-developed meshing tool, was used for the model creation of this project. The foundation system model geometries were acquired from pre-parameterized metrics set by the WP4 program. Model simplifications were made to the defined parameters in effort to reduce computational cost and allow for increased refinement near stress areas of interest.

The shallow gravity foundation R5L1/R5L2 and pile anchor R2L1/R2L2 meshes contain 556,200/668,848 and 138,132/977,788 elements respectively, shown in Figure 1 and Figure 2. To mitigate loading boundary effects, the soil was represented out a distance of 20 times the casing diameter and a depth of 1 times the respective embedment and pile anchor depth.

Axisymmetric geometry was implemented to reduce computational cost.

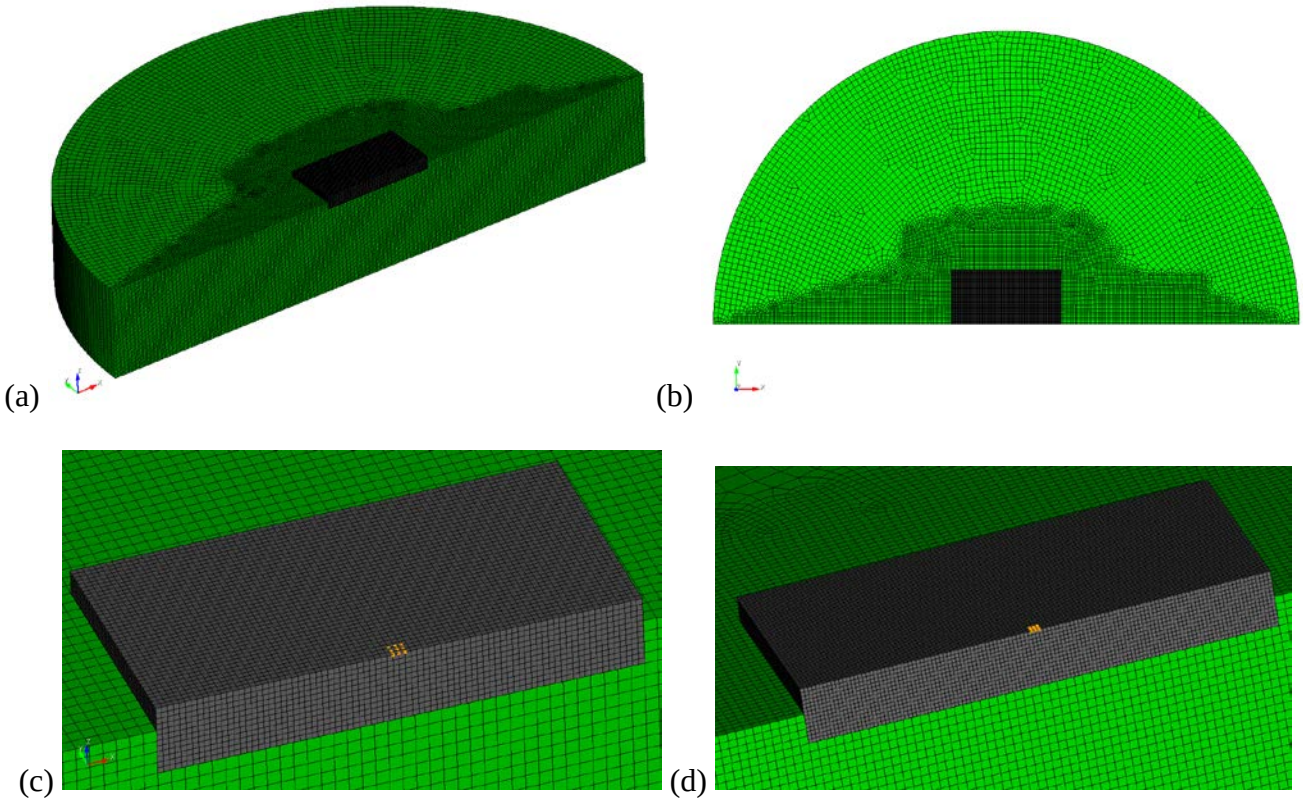

Figure 1: Full hex mesh of the shallow gravity foundation configuration shown in (a) isometric view (b) plan view and (c) load location of the representative anchor pad eye for R5L1 d) and R5L2

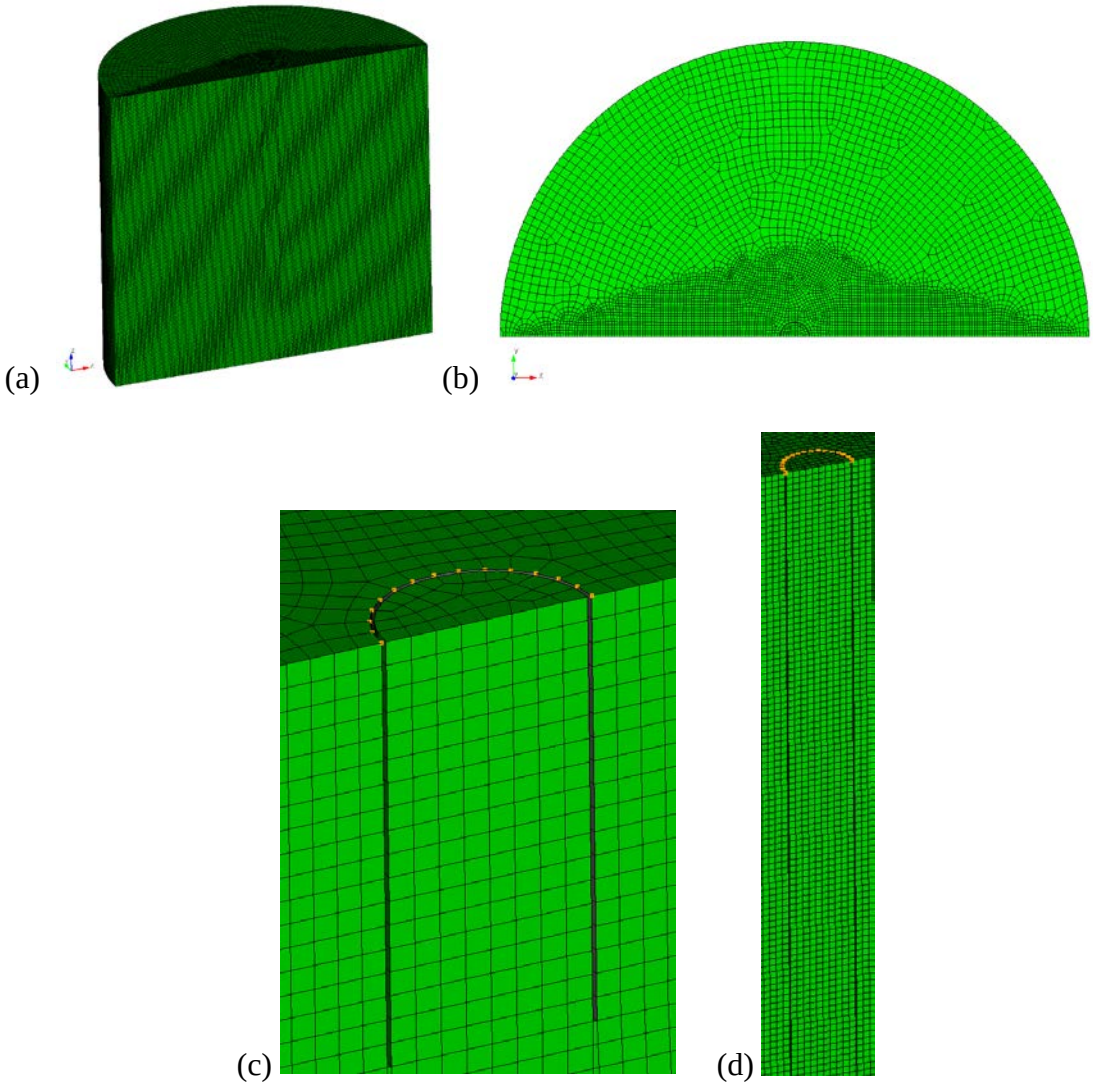

Figure 2: Full mesh of the pile anchor design configuration shown in (a) isometric view (b) plan view and (c) load location of the representative pile pad eye for R2L1 d) and R2L2

The mooring forces were applied to the shallow gravity foundation and pile anchor designs using nodeset boundary conditions, shown in Figure 1(c)-(d) and Figure 2 (c)-(d) respectively. The steel anchor components in the pile anchor design, by where the load was applied, utilized shell elements. These shells were lofted to their respective thickness, shown in Figure 3. Once the assemblies were created in CUBIT and exported in the genesis format, the Sierra/SM [2] code was used to perform subsequent analysis.

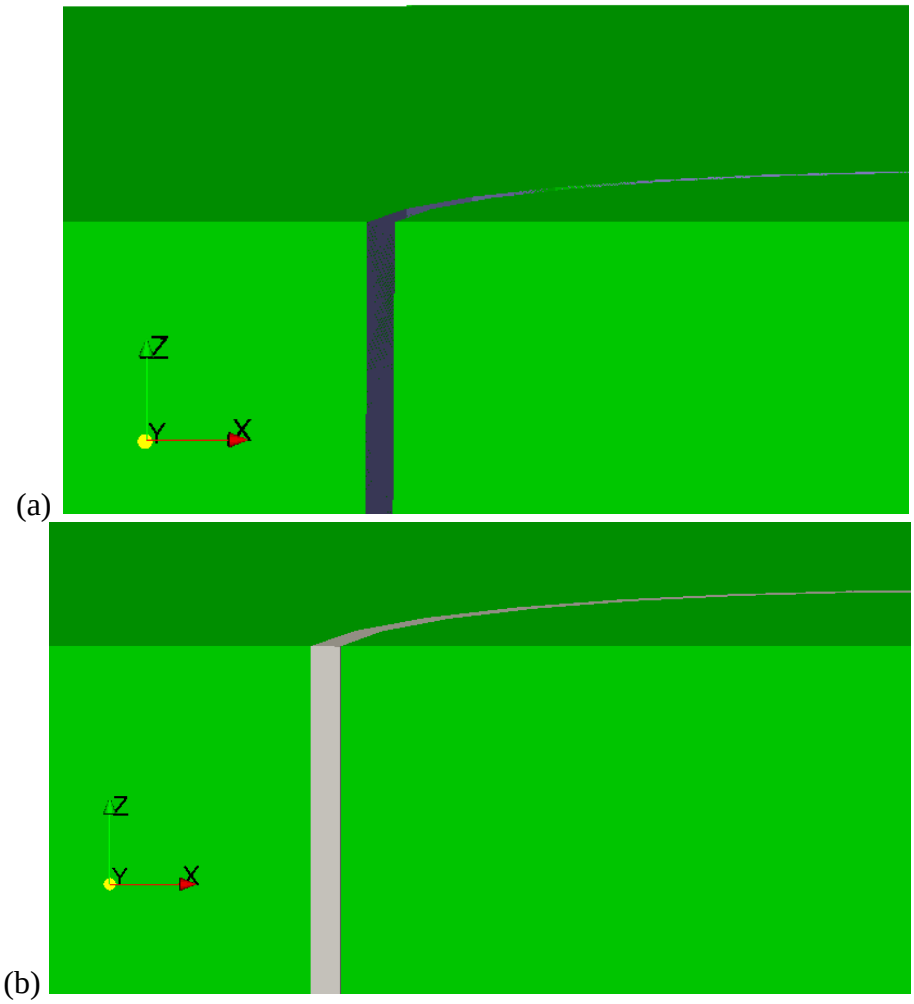

Figure 3: Shell elements were used to represent the thin pile anchor. For visualization, the pile anchor plate is shown in an (a) un-lofted (b) lofted configuration.

3. Materials and Methods

3.1. Soil and Crushable Foam Model

The soil and crushable foam material model was originally formulated by Krieg [1] and is currently implemented in Sierra/SM [2], based on PRONTO 3D [3]. The following 3.1 subchapter describing the function of this material model is an excerpt taken from PRONTO 3D [3]:

The yield surface assumed is a surface of revolution about the hydrostat in principal stress space as shown in Figure 4. In addition, a planar end capon the normally open end is assumed. The yield stress is specified as a polynomial in pressure, p (positive in compression)

$$\sigma_{yd} = a_0 + a_1 p + a_2 p^2 \quad (1)$$

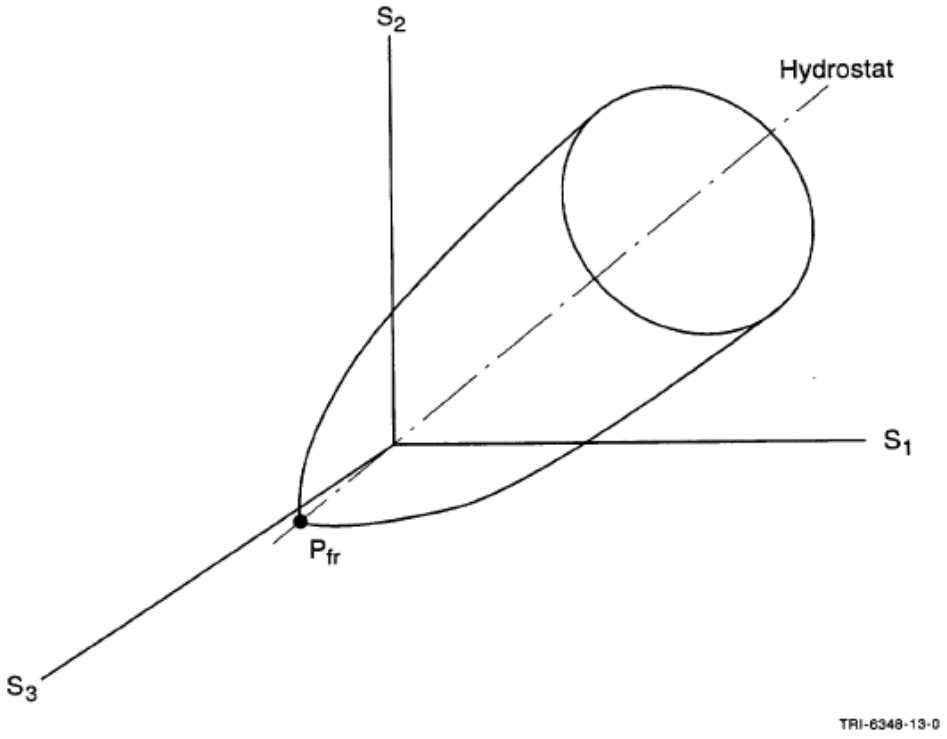

Figure 4: Pressure-dependent yield surface for the soils and crushable foams material model.

The determination of the yield stress from Equation 1 places severe restrictions on the admissible values of a_0, a_l, and a_2. There are three valid cases as shown in Figure 3. First, the user may specify a positive a_0, and a_1 and a_2 equal to zero as shown in Figure 5a. This gives an elastic-perfectly plastic deviatoric response, and the yield surface is a cylinder oriented along the hydrostat in principal stress space. Second, a conical yield surface (Figure 5b) is given by

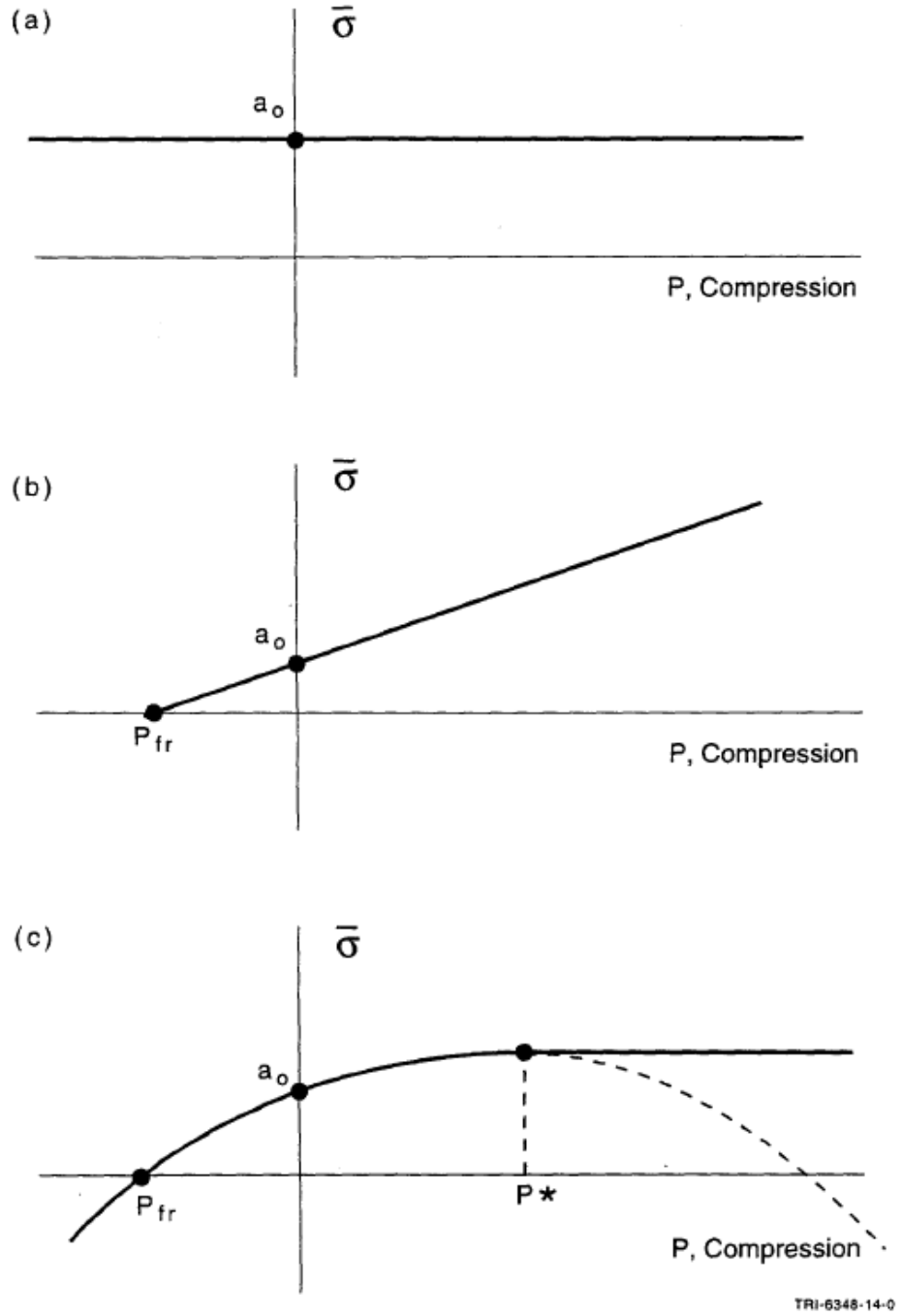

Figure 5: Forms of valid yield surface which can be defined for the soils and crushable foams material model.

setting a_2 to zero and entering appropriate values of a_0 and a_1. The program checks the user's input to determine whether a valid (negative) tensile fracture pressure, P_{fr}, results from the input data. The third case results when all three constants are nonzero and the program detects that a valid negative tensile failure pressure can be derived from the data. This case is shown in Figure 5c. A valid set of constants

for the third case results in a parabola as shown in Figure 5c. We have drawn the descending portion of the curve with a dashed line, indicating that the program does not use that portion of the curve. Instead, when the pressure exceeds P^*, the yield stress is held constant as shown at the maximum value.

The plasticity theories for the volumetric and deviatoric parts of the material response are completely uncoupled. The volumetric response is computed first. The mean pressure, p, is assumed to be positive in compression, and a yield function is written for the volumetric response as

$$\phi_p = p - f_p(\varepsilon_V) \tag{2}$$

where $f_p(\varepsilon_v)$ defines the volumetric stress-strain curve for the pressure as shown in Figure 6. This function is defined by the user with the restriction that the slope of the function must be less than or equal to the unloading bulk modulus, K_o, everywhere. If the user wishes the volumetric response to be purely elastic, he simply specifies no function identification (e.g., FUNCTION ID = 0). The yield function, ϕ_p, determines the motion of the end cap along the hydrostat.

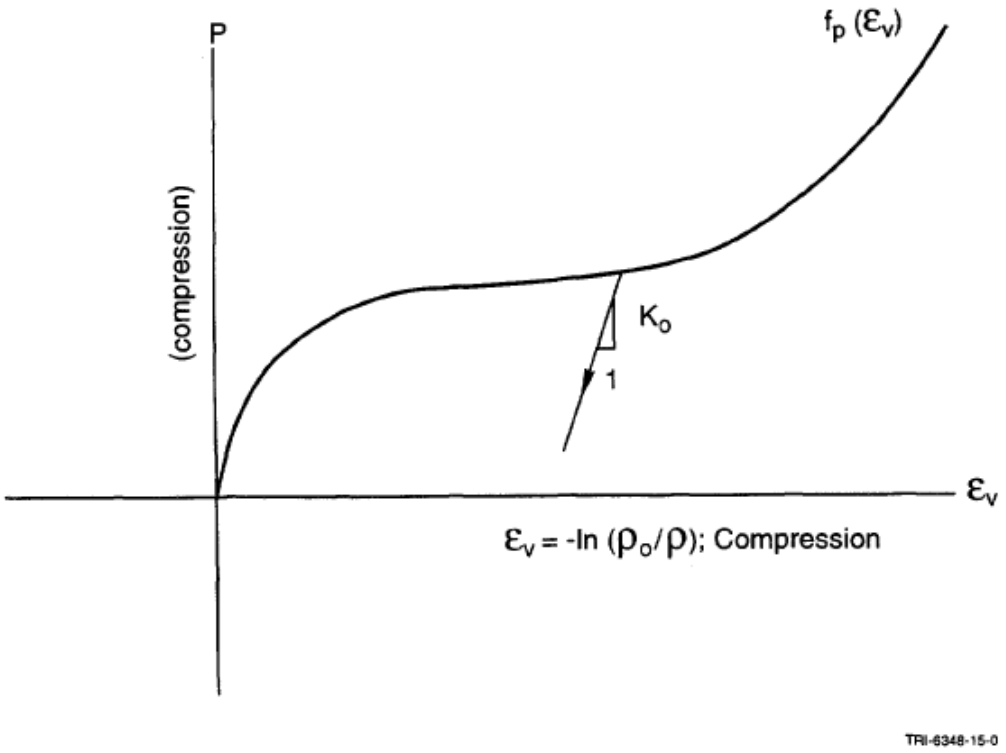

Figure 6: Pressure versus volumetric strain curve in terms of a user-defined curve, F(εv), for the soils and crushable foams material model.

The Soils and Crushable Foams model uses four internal state variables:

EVMAX - maximum compressive volumetric strain experienced (always positive),
EVFRAC - current value of volumetric fracture strain (positive in compression),
EV - current value of volumetric strain (positive in compression),
NUM - integer pointing to the last increment in the pressure function where the interpolate was found.

The PROP array (the input parameters for the soils and crushable foams model) contains the following entries for this material:

PROP(1) - 2μ
PROP(2) - Bulk Modulus, K_0
PROP(3) – a_0
PROP(4) – a_1
PROP(5) - a_2
PROP(6) - Function ID number.

3.2. Model Parameters

The anchor system design parameters used in the finite element analysis are shown in Table 2 and Table 3. The shallow gravity foundation pad eye was located in the middle of the anchor plate, axisymmetric across the cross-section.

Table 2: Shallow gravity foundation design parameters

Definition	units	Value: R5L1	Value: R5L2
Horizontal Load (x)	N	-1,088,723	3,977,200
Horizontal Load (y)	N	-924,297	-1,387,872
Vertical Load (z)	N	205,506	965,273
Foundation Width	m	12.33	18.76
Foundation Length	m	12.33	18.76
Foundation Height	m	0.65	1.07
Embedment Depth	m	1.23	1.88
Overburden pressure	Pa	1.177E+6	1.177E+6
Pad eye anchor length	m	0.305	0.305
Pad eye anchor width	m	0.305	0.305

Table 3: Pile anchor design parameters

Definition	units	Value: R2L1	Value: R2L2
Horizontal Load (x)	N	-1,088,723	3,977,200
Horizontal Load (y)	N	-924,297	-1,387,872
Vertical Load (z)	N	205,506	965,273
Pile Diameter	m	3.00	3.50
Pile Grout Diameter	m	0	0
Pile Length	m	6	32
Pile Thickness	m	0.06	0.06
Overburden pressure	Pa	1.177E+6	1.177E+6

The material properties used to parameterize the FE model are shown in Table 4. The shallow gravity foundation and pile anchor designs implemented the soft clay soil and foam material model parameters. All anchor systems utilized identical steel properties.

Table 4: Material model parameters

Definition	Units	Soft Clay	Steel
Density	$\frac{kg}{m^3}$	1,762	7,860
Young Modulus	Pa	13.41E+6	1.999E+11
Poisson's Ratio	-	0.45	0.3
A0	Pa	35910	-
A1	Degrees	0	-
A2	Degrees	0	-
Yield Stress	Pa	-	427.7E+6

3.3. Loading and Boundary Conditions

The simulation approach implemented the loadings described in the model dimensions and loading levels denoted in Table 2 and Table 3. Both anchor systems applied the pad eye load evenly distributed across pad eye anchor. This was accomplished by dividing the prescribed load across the respective node surface of the pad eye. The soil mass bottom faces were fixed in the vertical direction, the front cross section faces were fixed normal to their surfaces, and the outer circumferential surfaces of the soil mass were allowed to move only in the vertical orientation. Sierra/SM [2] explicit quasistatic mode solver was utilized for these simulations. A uniform seafloor friction coefficient of 0.5 was implemented in the design studies.

4. Results

Contour plots of Von Mises stress, Equivalent Plastic Strain (EQPS), and Maximum Compressive Volumetric Strain (EVMAX) are shown in Figure 8 through Figure 13 for the shallow gravity foundation and Figure 15 through Figure 20 for the pile anchor designs. Non-magnified displacements are shown in these figures. Midsection slice locations of the shallow gravity foundations are denoted by the red line shown in Figure 7 and in Figure 14 for the pile anchor designs.

The shallow gravity foundation R5L1 design results show the Von Mises stress reaches a maximum of approximately 36E3 Pa uniformly distributed across the soil volume principally due to the overburden pressure and a significant stress relief directly under the shallow foundation load application. Localized plastic strain is present at the foundation corners, reaching approximately 0.5 EQPS and averaging approximately 0.25 EQPS in the nearby surrounding soft clay bordering the anchor. The EQPS quickly dissipates to zero around the outer surrounding clay mass. Maximum compressive volumetric strain for the shallow foundation design reaches 0.03 and occurs in the surrounding soil.

The shallow gravity foundation R5L2 design results shows similar Von Mises stress of 36E3 Pa uniformly distributed across the soil volume and a significant stress relief on the bottom left of the foundation load application; a change due to the altered horizontal and vertical load resultant vector produced in R5L2. Localized plastic strain is present at the foundation corners, reaching approximately 1.0 EQPS and averaging approximately 0.5 EQPS in nearby surrounding soft clay bordering the anchor. Maximum compressive volumetric strain for the anchor design reaches 0.03 and occurs in the surrounding foundation soil.

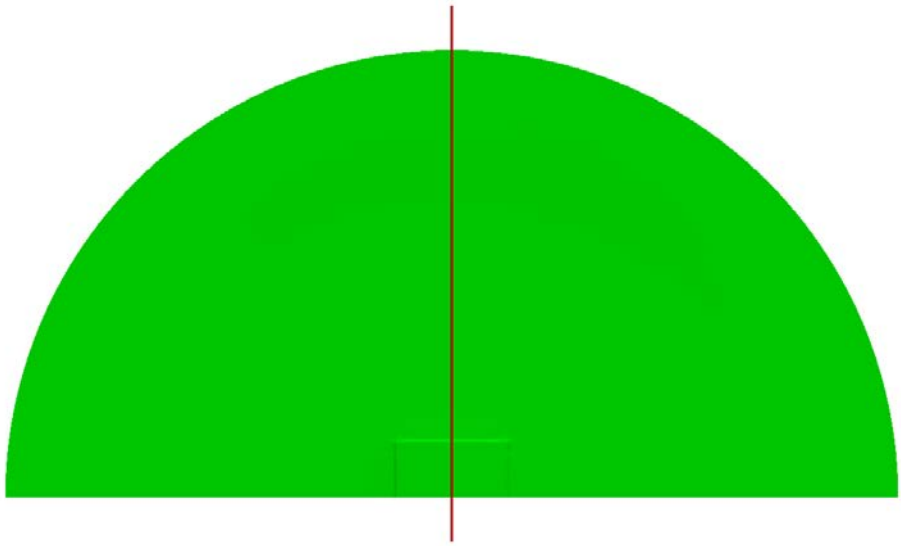

Figure 7: Plan view of the shallow gravity foundation denoting midsection slice location.

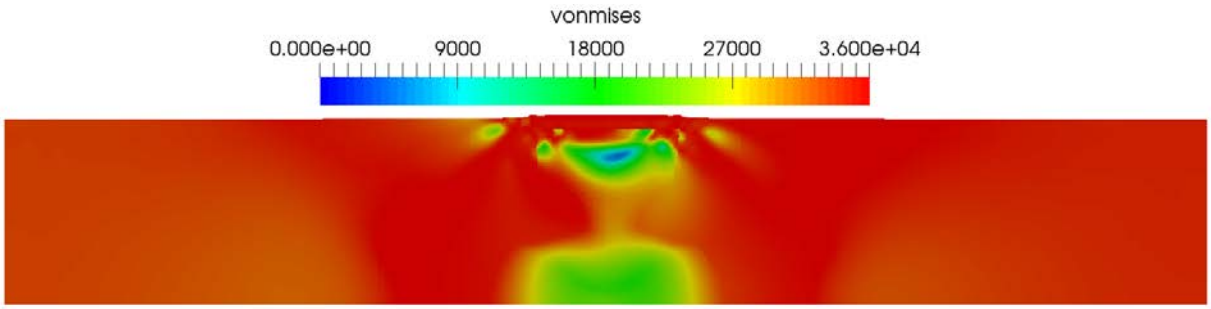

(a)

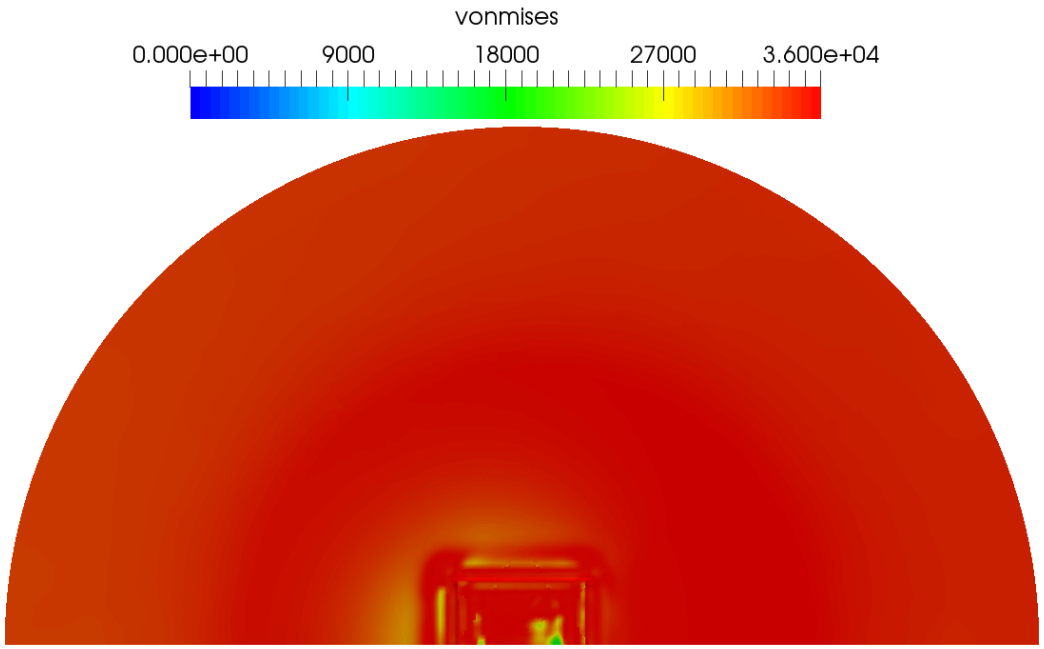

(b)

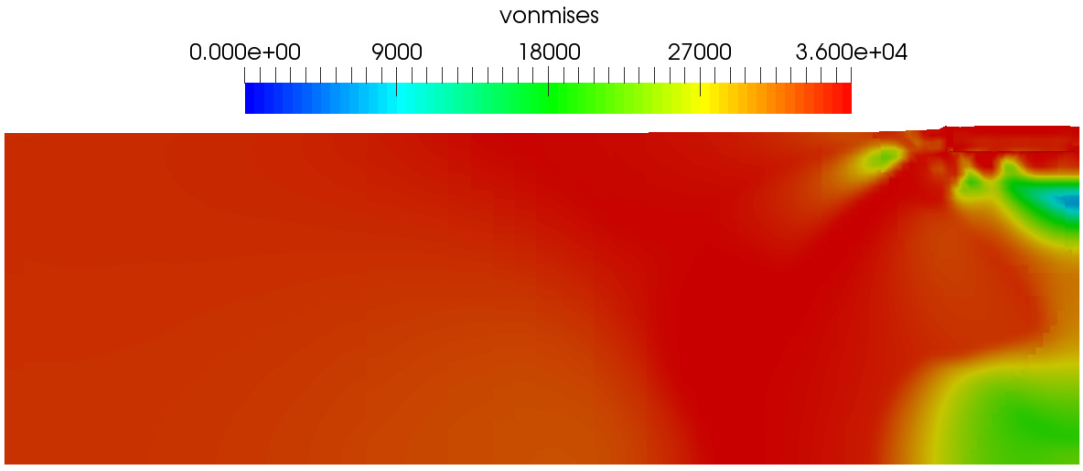

(c)

Figure 8: Von Mises stress (Pa) shown in (a) front view (b) plan view and (c) sliced midway through the shallow gravity foundation R5L1.

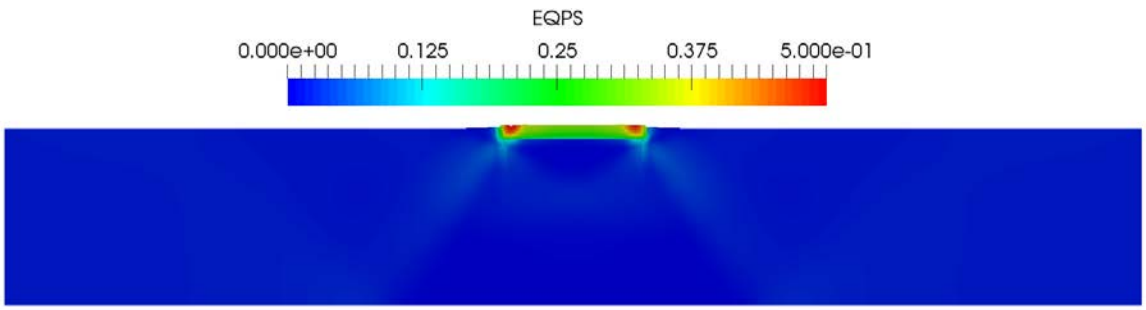

(a)

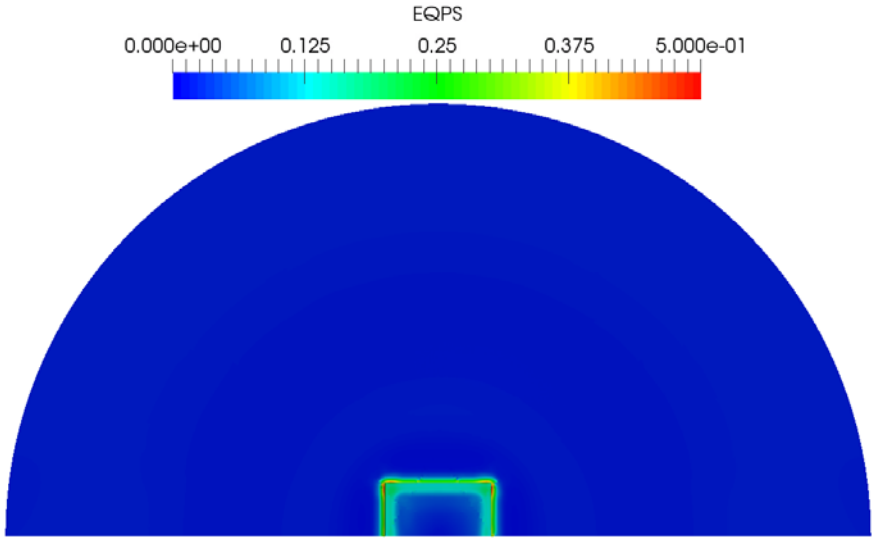

(b)

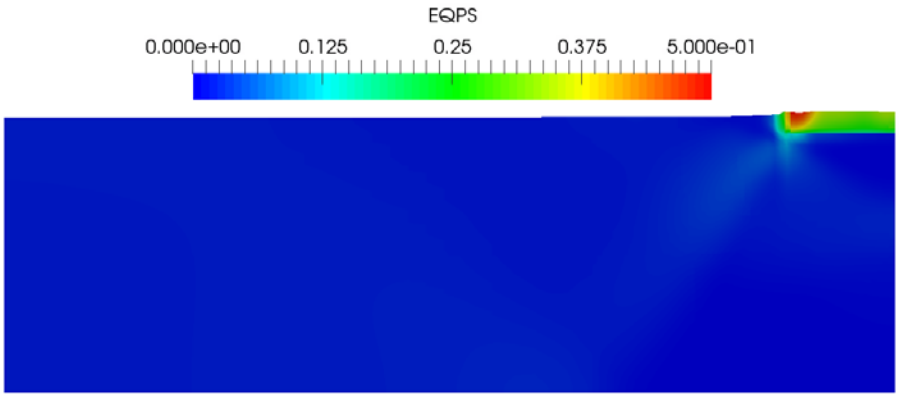

(c)

Figure 9: EQPS shown in (a) front view (b) plan view and (c) sliced midway through the shallow gravity foundation R5L1.

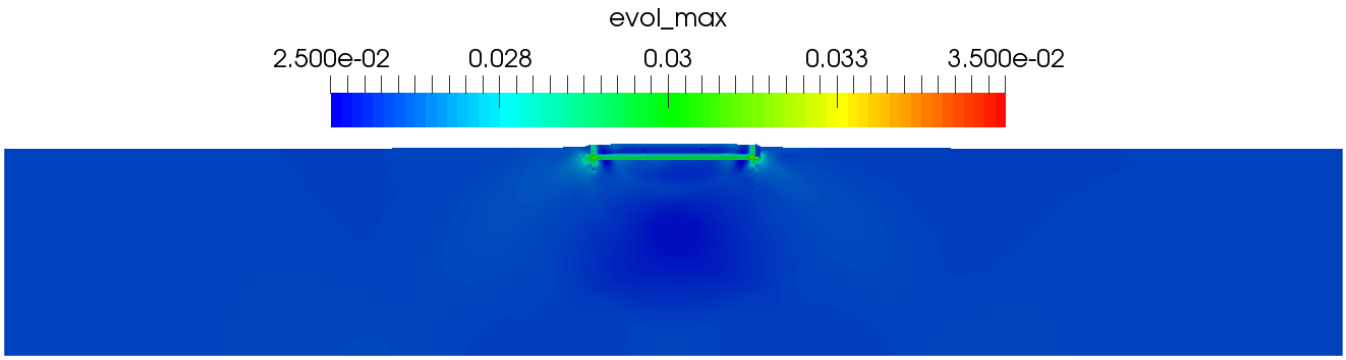

(a)

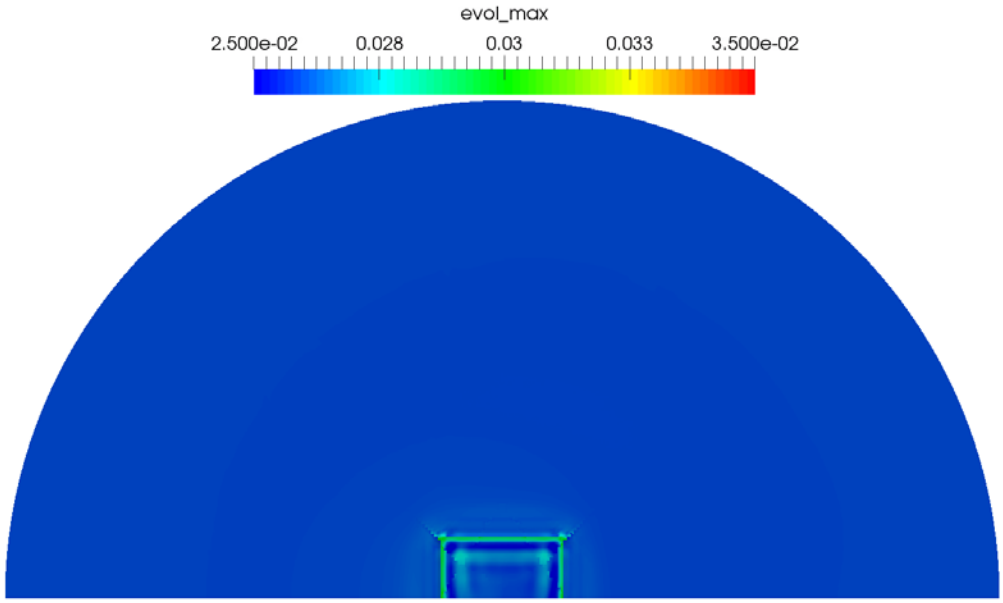

(b)

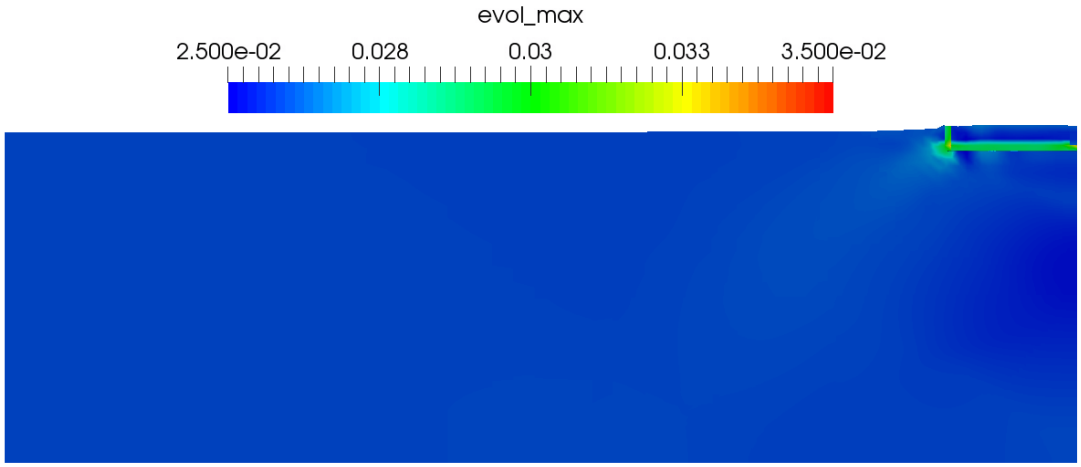

(c)

Figure 10: Maximum compressive volumetric strain shown in (a) front view (b) plan view and (c) sliced midway through the shallow gravity foundation R5L1.

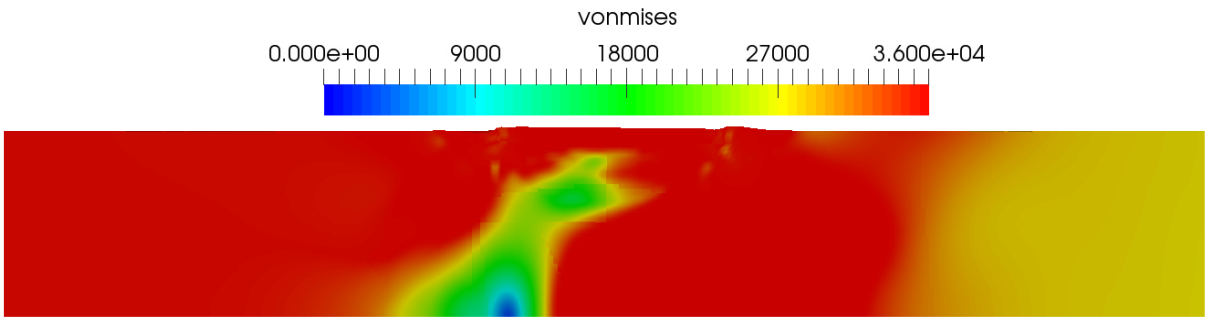

(a)

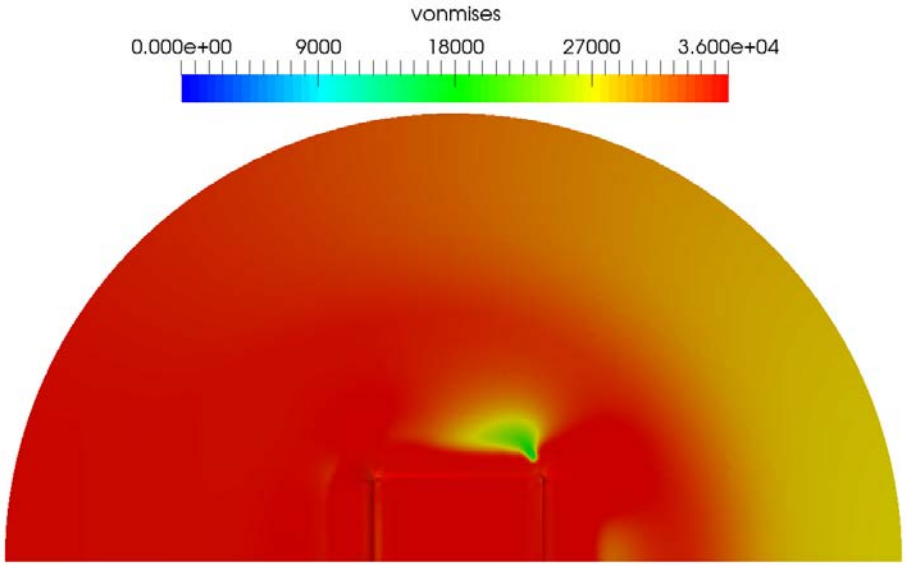

(b)

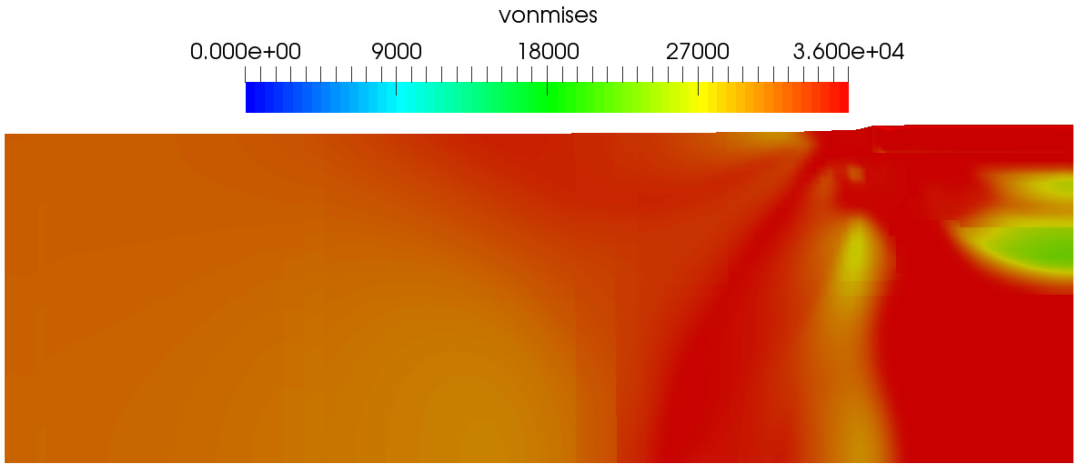

(c)

Figure 11: Von Mises stress (Pa) shown in (a) front view (b) plan view and (c) sliced midway through the shallow gravity foundation R5L2.

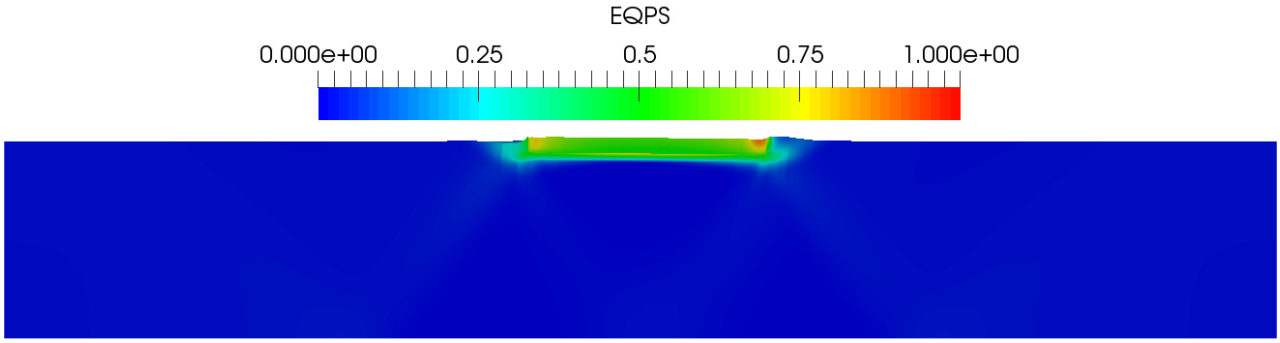

(a)

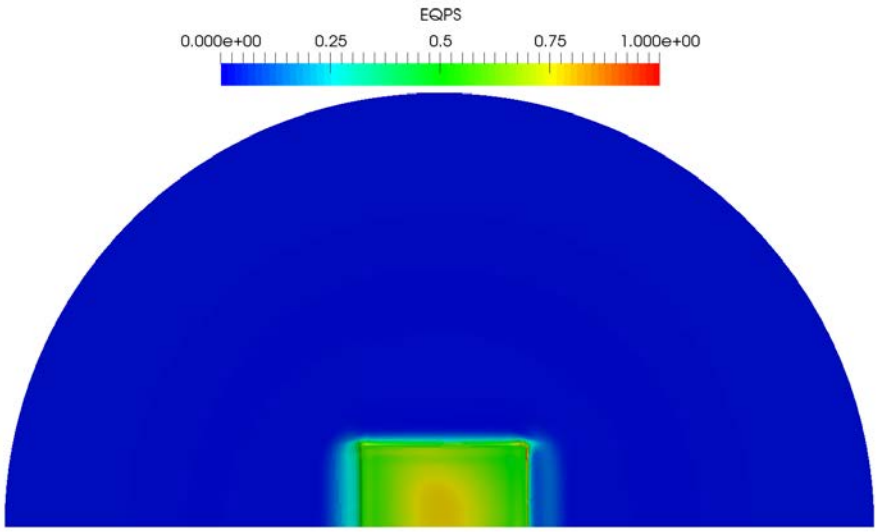

(b)

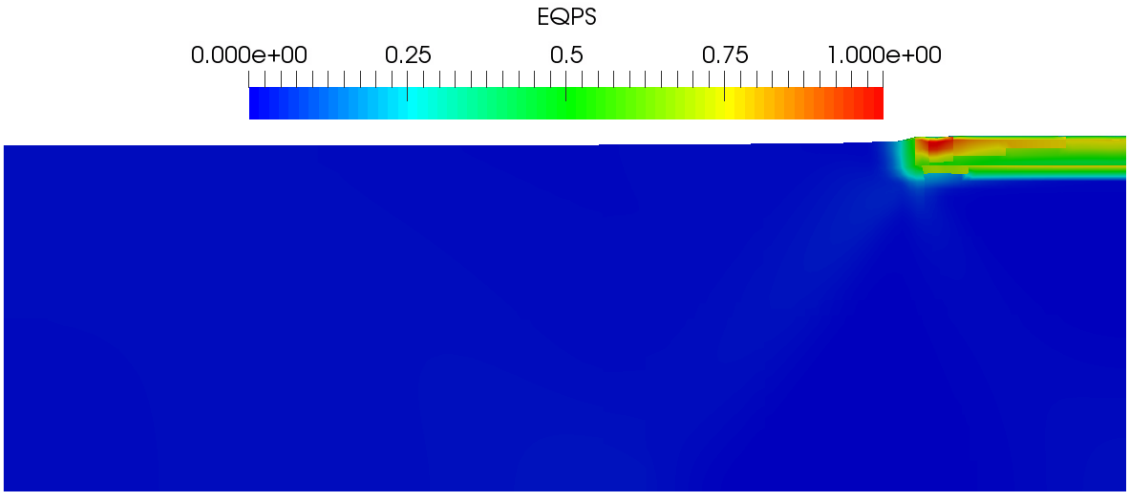

(c)

Figure 12: EQPS shown in (a) front view (b) plan view and (c) sliced midway through the shallow gravity foundation R5L2.

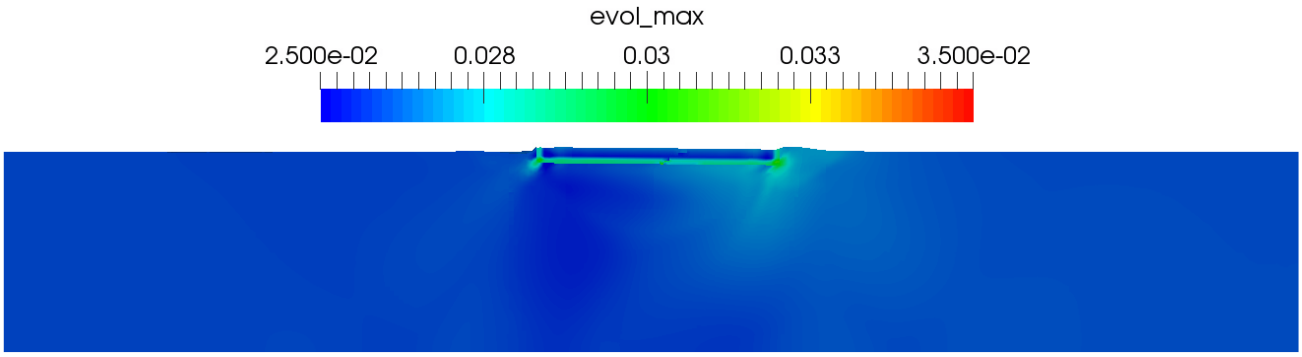

(a)

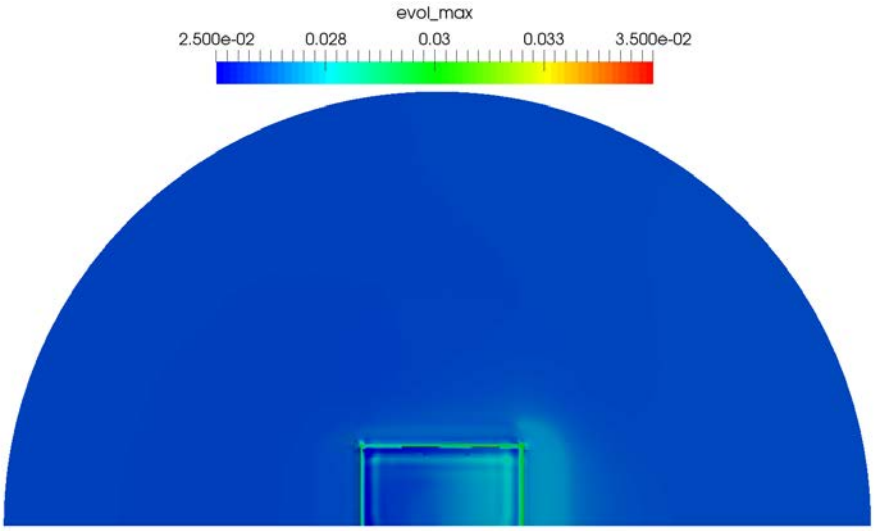

(b)

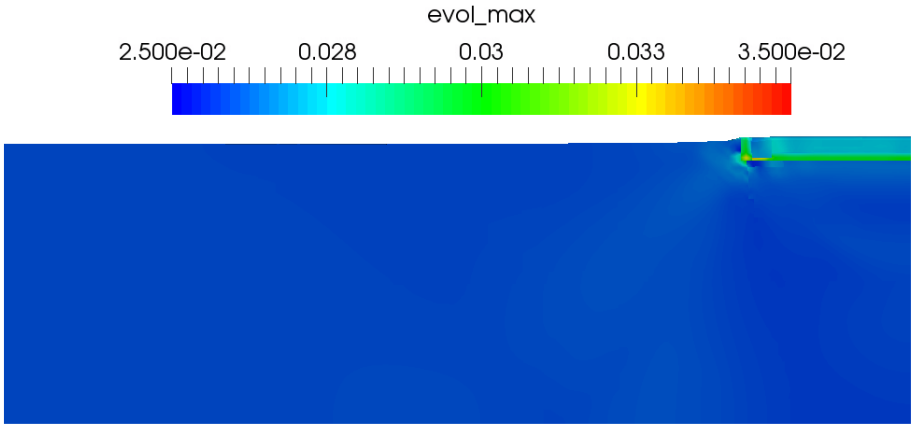

(c)

Figure 13: Maximum compressive volumetric strain shown in (a) front view (b) plan view and (c) sliced midway through the shallow gravity foundation R5L2.

The pile anchor R2L1 design results shows Von Mises stress of 36E3 Pa uniformly distributed across the soil volume principally due to the overburden pressure and a significant stress relief below the pile anchor opposite of the resultant vector load. The highest localized plastic strain occurs at the surface edge of the pile, reaching approximately 0.7 EQPS, averaging around 0.35 EQPS in the soft clay around the pile anchor, and dissipating to zero around the surrounding soil volume. Maximum compressive volumetric strain for the pile design reaches 0.03, localized in the left soil surface in contact with the counter-clockwise overturning pile anchor.

The pile anchor R2L2 design results shows similar Von Mises stress of 36E3 Pa uniformly distributed across the soil volume and various hotspots of stress relief around clockwise the overturning pile anchor. Similarly to R2L1, high localized plastic strain occurs at the surface edge of the pile anchor, reaching approximately 2.0 EQPS, averaging around 1.0 EQPS in the soft clay around the pile anchor, and dissipating to zero around the surrounding soil volume. Maximum compressive volumetric strain for the pile design reaches 0.03 on the upper right and lower left of the pile anchor and a minimum of 0.015 in the mid-section of soil along the inner pile. A significant source of volumetric stress and strain shown in the shallow gravity foundation and pile anchor designs is induced by the constant overburden pressure of 1.18E6 Pa.

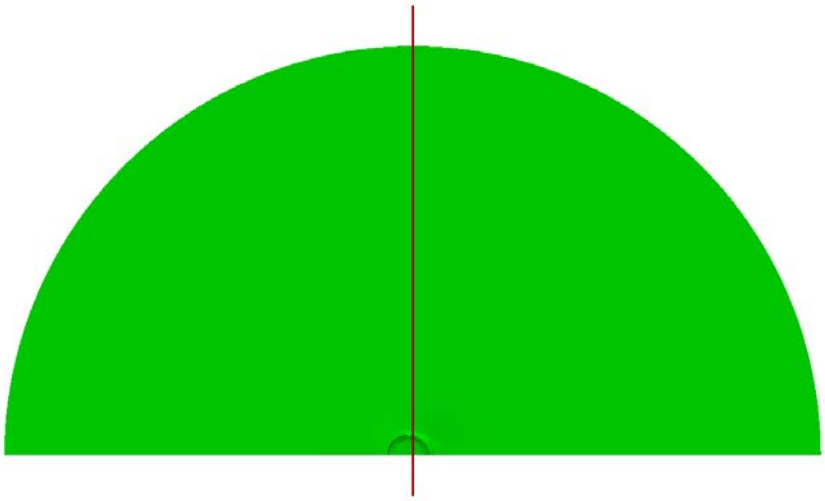

Figure 14: Plan view of the pile anchor foundation denoting midsection slice location.

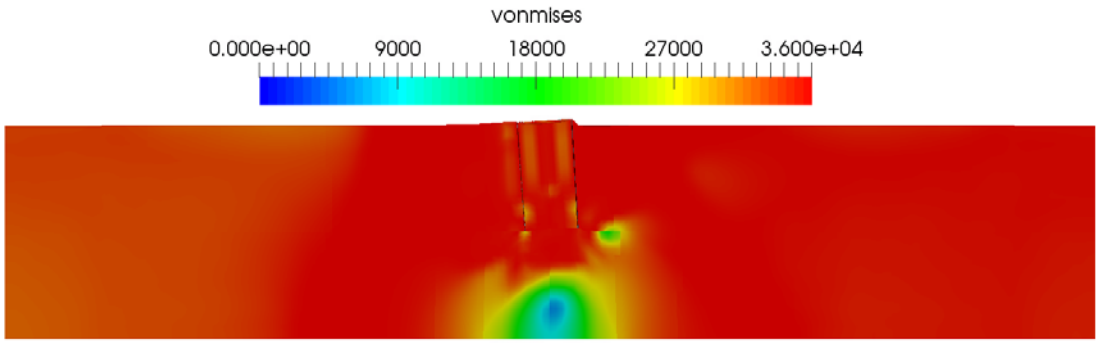

(a)

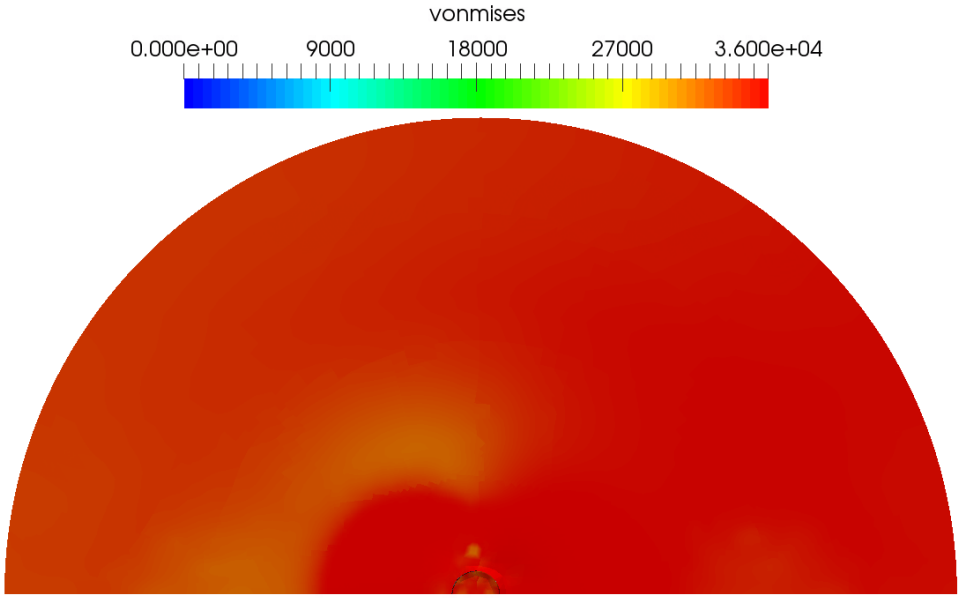

(b)

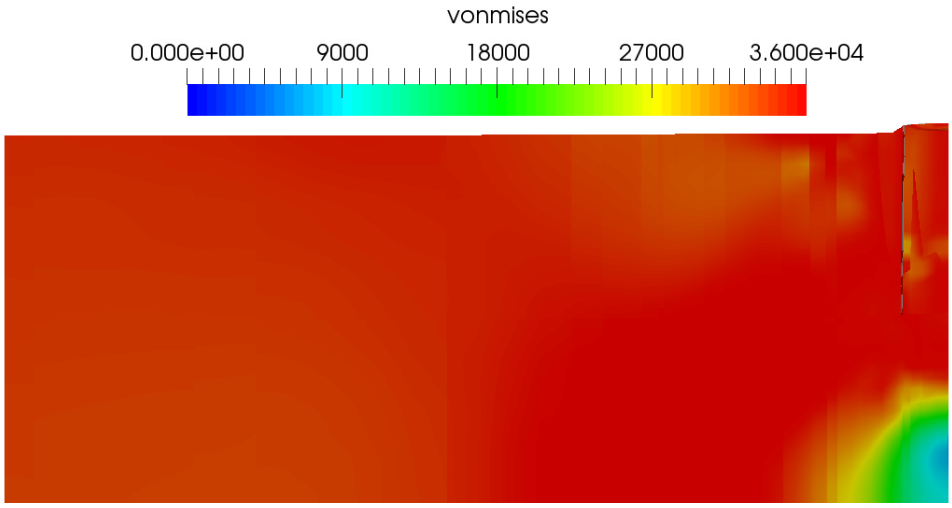

(c)

Figure 15: Von Mises stress (Pa) shown in (a) front view (b) plan view and (c) sliced midway through the pile anchor R2L1.

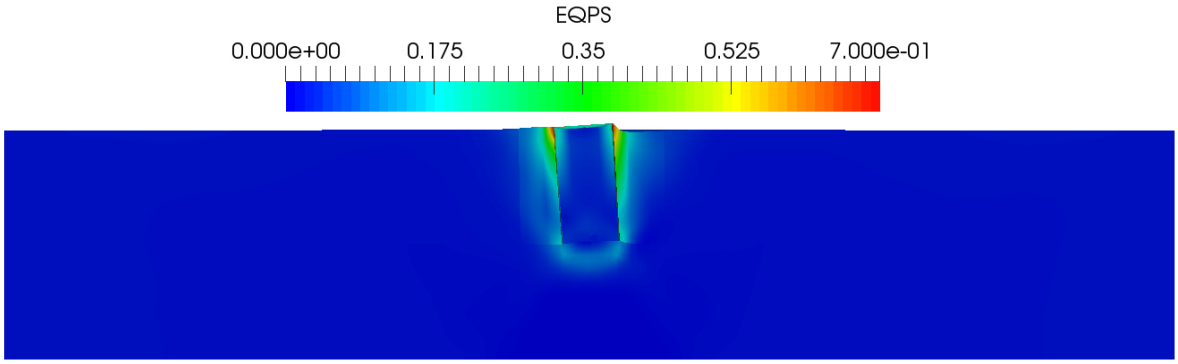

(a)

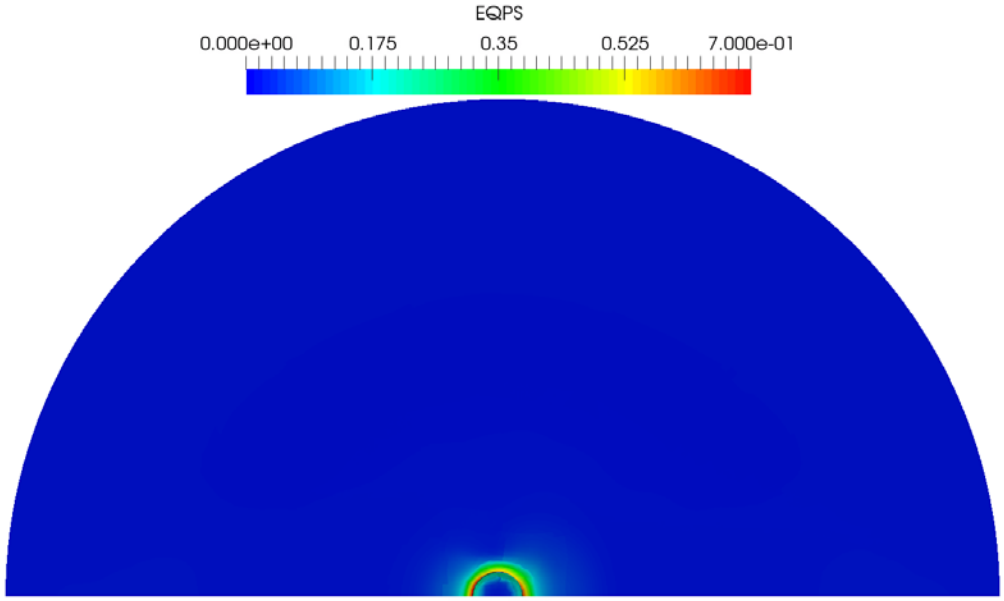

(b)

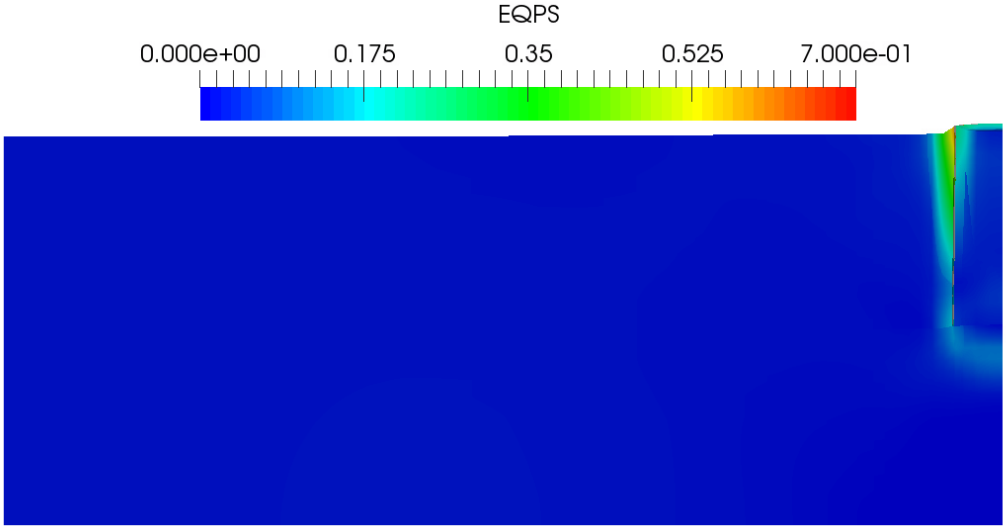

(c)

Figure 16: EQPS shown in (a) front view (b) plan view and (c) sliced midway through the pile anchor R2L1.

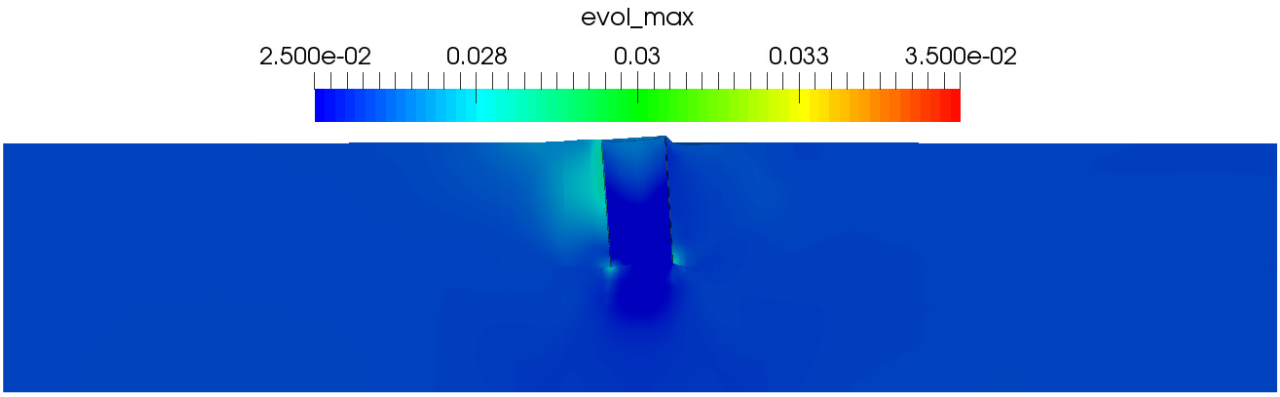

(a)

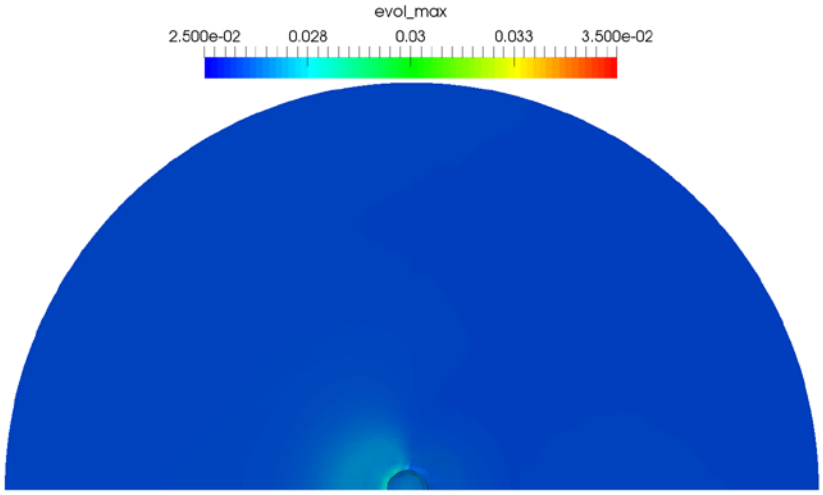

(b)

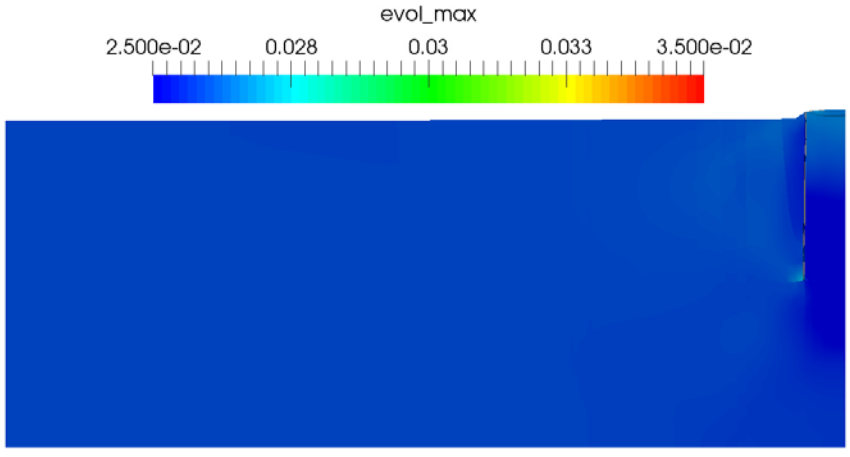

(c)

Figure 17: Maximum compressive volumetric strain shown in (a) front view (b) plan view and (c) sliced midway through the pile anchor R2L1.

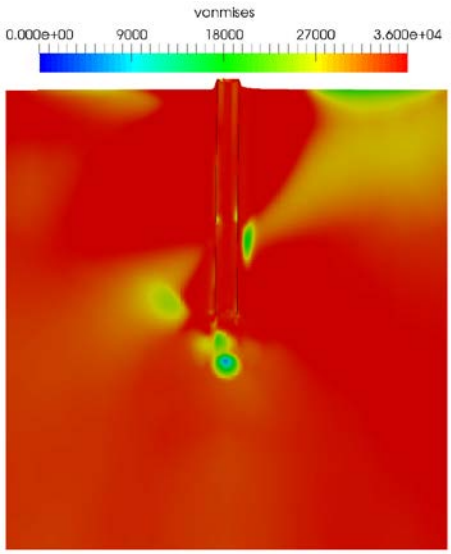

(a)

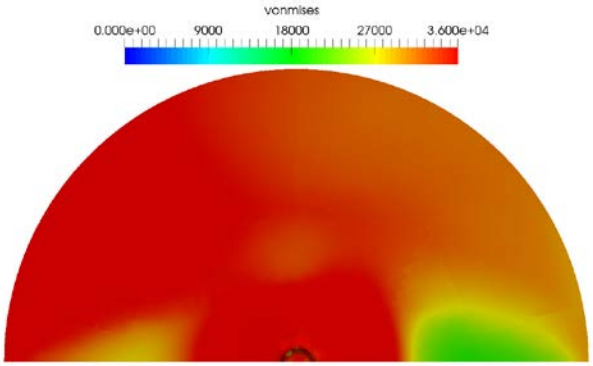

(b)

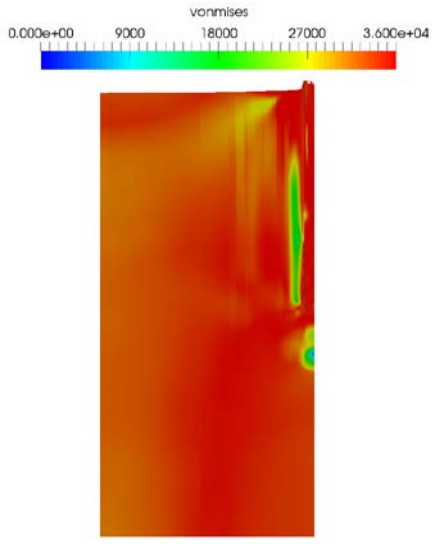

(c)

Figure 18: Von Mises stress (Pa) shown in (a) front view (b) plan view and (c) sliced midway through the pile anchor R2L2.

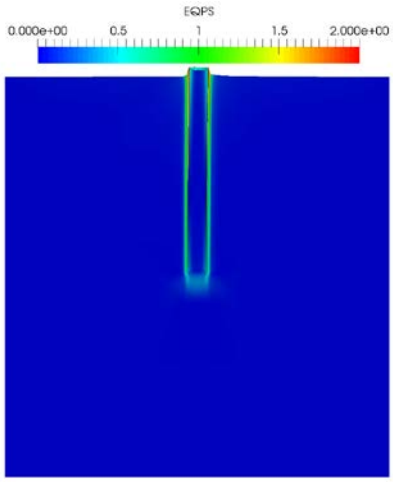

(a)

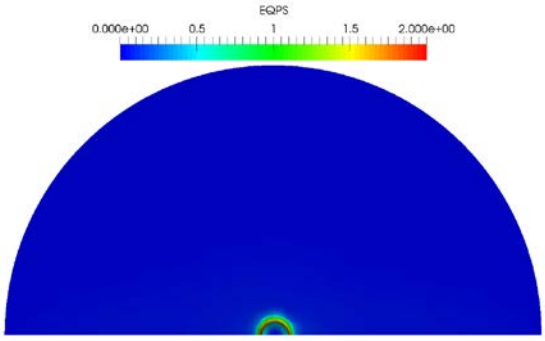

(b)

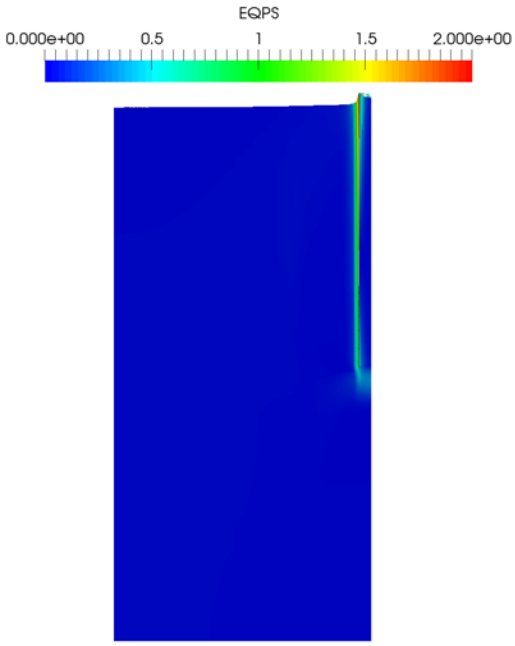

(c)

Figure 19: EQPS shown in (a) front view (b) plan view and (c) sliced midway through the pile anchor R2L2.

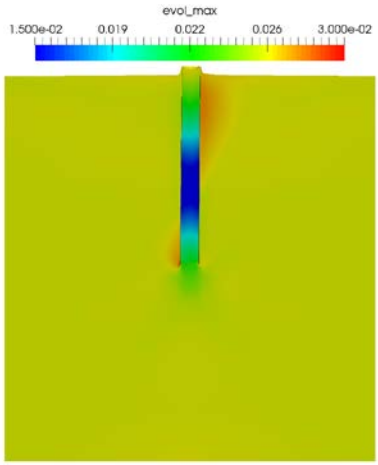

(a)

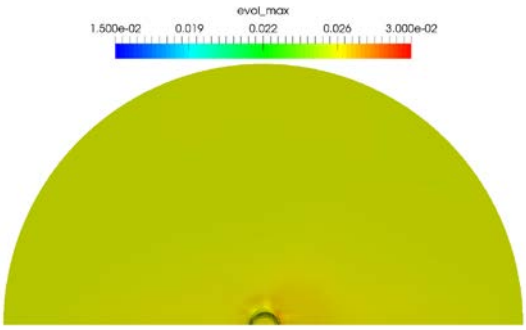

(b)

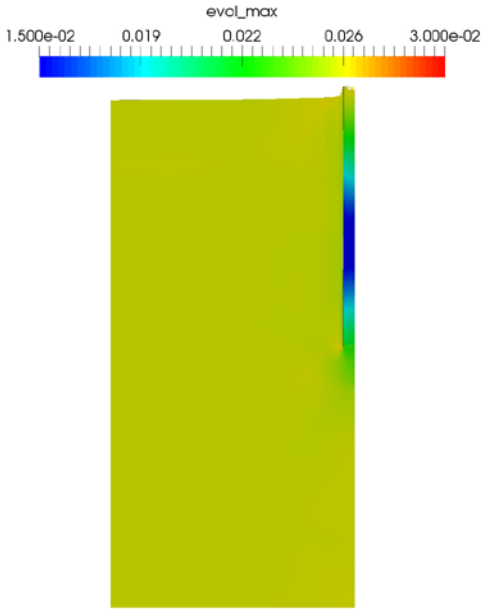

(c)

Figure 20: Maximum compressive volumetric strain shown in (a) front view (b) plan view and (c) sliced midway through the pile anchor R2L2.

5. Conclusions and Future Work

The shallow gravity foundation and pile anchor designs show localized stress and strain under the prescribed loading conditions, but the respective soft clay soil mass does not fail throughout the soil volume. The proposed designs should provide as adequate anchor systems for the respective load scenarios proposed.

As mentioned in the prior DTOcean foundation and anchor study [4], further review and refinement of the WP4 program material conversion to the Sierra/SM [2] soil and foam material model is desired. Additionally, the physical loading process of these anchors should be better understood to replicate FE boundary conditions with higher fidelity. Field data and/or data from NAVFAC based analytic tools would provide a means of model comparison and potentially allocate a baseline calibration model. Further FEA is recommended for exploring model sensitivity and parameter range variability such as load magnitude, load application site, and soil material definition.

Internal Distribution

MS-0346	S. Gomez	Org. 01556
MS-1124	J. Roberts	Org. 06122
MS-0751	R. Jensen	Org. 06914
MS-0750	J. Heath	Org. 06914
MS-0828	M. Ross	Org. 01557
MS-0346	D. Peebles	Org. 01556
MS-0735	M. Lee	Org. 06914

Acknowledgments

This work was funded by the Department of Energy’s (DOE) Energy Efficiency and Renewable Energy (EERE) Program’s Wind and Water Power Technologies Office.

Sandia National Laboratories is a multi-program laboratory managed and operated by Sandia Corporation, a wholly owned subsidiary of Lockheed Martin Corporation, for the U.S. Department of Energy's National Nuclear Security Administration under contract DE-AC04-94AL85000. SAND Number: 2013-6867 C.

References

1. Krieg, R.D., (1978) "A Simple Constituive Description for Soils and Crushable Foams," SC-DR-72-0883. Albuquerque, NM and Livermore, CA: Sandia National Laboratories.
2. SIERRA Solid Mechanics Team (2016). Sierra/SolidMechanics 4.40 User’s Guide. SAND Report 2016-2707. Albuquerque, NM and Livermore, CA: Sandia National Laboratories.
3. Taylor L.M. and Flanagan, D.P., (1989). Pronto 3D A Three-Dimensional Transient Solid Dynamics Program: SAND87-1912. Albuquerque, NM and Livermore, CA: Sandia National Laboratories.
4. Gomez, S.P., Jensen, R.P., Heath, J.E. (2016) An Investigation of DTOcean Foundation and Anchor Systems. SAND Report 2016-6076 O. Albuquerque, NM and Livermore, CA: Sandia

National Laboratories.

Attachments

foundationvalidation.xlsx